

# Double-grating-structured light microscopy using plasmonic nanoparticle arrays

S. Liu,<sup>1</sup> Chin-Jung Chuang,<sup>1</sup> C. W. See,<sup>1</sup> G. Zorinians,<sup>2</sup> W. L. Barnes,<sup>2</sup> and M. G. Somekh<sup>1,\*</sup>

<sup>1</sup>*Institute of Biophysics and Optical Science, Department of Electrical and Electronic Engineering, University Park, University of Nottingham, NG7 2RD, UK*

<sup>2</sup>*School of Physics, University of Exeter, Stocker Road, Exeter, Devon, EX4 4QL, UK*

\*Corresponding author: [mike.somekh@nottingham.ac.uk](mailto:mike.somekh@nottingham.ac.uk)

Received November 12, 2008; revised February 12, 2009; accepted February 14, 2009;  
posted March 9, 2009 (Doc. ID 104061); published April 10, 2009

Structured illumination increases the spatial bandwidth of optical microscopes. We demonstrate bandwidth extension using a physical grating placed close to the sample. This comprises an array of elongated nanoparticles, whose localized surface plasmon resonance is polarization dependent. By arranging the particle orientation to vary with position the grating can be moved by changing the input polarization. A projected optical grating provides an additional independent mechanism for bandwidth extension. Experimental results showing bandwidth improvement in one direction are presented, and the measures necessary to extend the technique for routine imaging are discussed. © 2009 Optical Society of America

OCIS codes: 180.2520, 180.4243, 050.6624, 110.4850, 250.5403, 350.5730.

Structured illumination fluorescence microscopy (SIM) is a technique [1] that improves the lateral resolution of widefield microscopy. The essential ideas are summarized in [2]. The technique involves illuminating the sample with an optical grating; this mixes the object spatial frequencies with the grating frequency so that wave-vector components that are not normally passed through the objective lens are down-converted into its passband. The spatial Fourier transform of the measured image is a superposition of high- and low-frequency components; to separate them the grating is moved, typically, three or four phase steps. The final image may then be recovered by taking the inverse Fourier transform of the newly synthesized spatial frequency map.

In its linear form SIM, at best, doubles the bandwidth compared with a conventional fluorescence microscope; this limit arises from the far-field nature of the projected grating. Heinzmann *et al.* [3] have proposed nonlinear SIM involving saturation of fluorophores. This distorts the excitation profile and creates higher-order spatial frequency components, allowing better resolution. To avoid saturating the fluorophore, which can induce photobleaching, the idea of using a movable physical grating has been studied theoretically [4,5]. Since the physical grating is near the sample, its periodicity is not limited by diffraction through the illuminating optics; it can thus enhance the resolution to a greater degree than the optical grating. Experimentally, physical gratings have been used for nonfluorescent microscopy [6]. In this Letter we show a narrowed point-spread-function (PSF) using a physical grating in a fluorescent microscope.

The physical grating used here relies on the localized surface plasmon resonance (LSPR) of gold nanoparticles. When the frequency of light matches the LSPR the incident electric field is enhanced and confined to a small volume. Combining physical and optical gratings gives an even larger spatial frequency enhancement, as these mix to produce sum and

difference frequencies. We call this system a double-grating structured-illumination microscope (DGSIM). The experimental results demonstrate the feasibility for substantial improvement in spatial bandwidth and introduce the key ingredients to develop this concept. The proof-of-concept results were obtained with a modest NA and in only one dimension. We conclude by discussing approaches that will extend the results so that it can be applied to routine imaging.

Figure 1 shows the optical arrangement. The source was a 633 nm He-Ne laser whose polarization is controlled using a half-wave plate. The optical grating is placed conjugate with the object plane. A spatial filter is placed in the Fourier plane  $F_1$  to block undesired orders (such as the zero order). The physical grating (B) was illuminated through a microscope objective. The sample substrate consists of a cover-glass with gold nanostructures arranged as shown in Fig. 1. The gold nanoparticles were produced by electron-beam lithography [6] with dimensions of 125 nm × 35 nm and a thickness of 40 nm. In the array, the long axis of each nanoparticle is rotated by 45° in successive columns; a complete cycle (180°) is achieved every four particles. At the incident wavelength (633 nm) the longitudinal resonance of the particles dominates the transverse resonance so that the field enhancement close to the particle is far

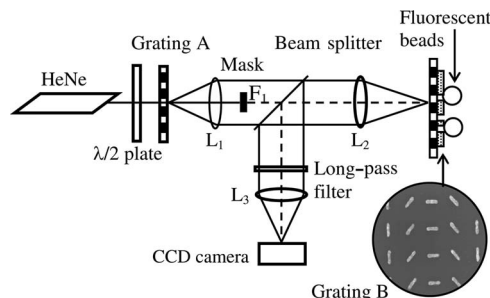


Fig. 1. Schematic of the optical setup. Inset, electron micrograph of the physical grating; period = 1 μm.

greater when the incident polarization is oriented along the long axis.

To demonstrate the spatial phase shifting the grating was covered with a thin uniform polymer layer (30-nm-thick PMMA, 950kD) containing 2 wt. % of the fluorescent dye Oxazine 1 perchlorate. This dye has been shown to exhibit enhanced emission when excitation is mediated by LSPR. It has been shown that the dye is evenly dispersed in PMMA and follows the profile of the nanoparticles [7]. The fluorescence image from the grating comprised parallel stripes. Figure 2 shows the spatial phase of the stripes as polarization of the incident light was rotated, corresponding to grating movement. Phase shifting of the optical grating was achieved by moving the optical grating (grating A of Fig. 1) with a motorized scan stage.

The reconstruction of higher-resolution images is an extension of the standard routine outlined above. We obtained nine images by moving the optical grating to its first position then taking three images with the waveplate at three different angles,  $60^\circ$  apart; this process was then repeated for two further positions of the optical grating.

Assuming sinusoidal illumination patterns (we discuss the implications of this assumption later) the combination of the two gratings can be represented by

$$I_{mn}(x) = [1 + g_o \cos(k_o x + \phi_m)] \times [1 + g_p \cos(k_p x + \psi_n) + \dots], \quad (1)$$

where  $g_o$ ,  $g_p$ ,  $k_o$ , and  $k_p$  are the modulation depths and  $k$  vectors of the two gratings, respectively.  $\phi_m$  and  $\psi_n$  are the  $m$ th and  $n$ th phase shifts of the gratings. When a sample,  $S(x)$ , is illuminated by  $I_{mn}(x)$  the output signal,  $O_{mn}(x)$  is given by

$$O_{mn}(x) = [I_{mn}(x)S(x)] \otimes H(x), \quad (2)$$

where  $H(x)$  is the PSF of the microscope and  $\otimes$  is the convolution operator. This means that the microscope objective passes spatial frequencies associated with the object ("spectral orders") that would normally not be passed through the lens. These spectral orders represent frequency components displaced by  $pk_o + qk_p$ , where  $p$  and  $q$  take values (for sinusoidal exci-

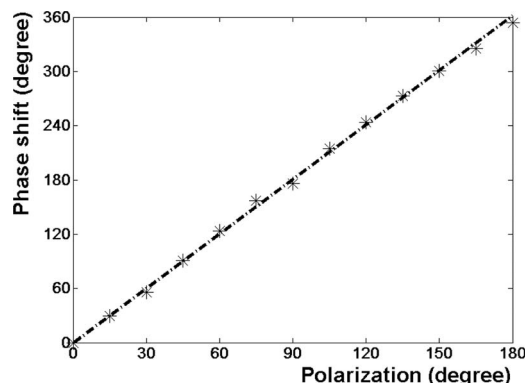


Fig. 2. Optical phase shift of light beam after passing through the physical grating, as a function of the polarization angle of the incident beam.

tation) of  $-1$ ,  $0$ , and  $1$ , resulting in a total of nine spectral orders. We separate these terms with the series of phase steps described above, which establishes a set of nine linear equations that are solved by inverting the matrix. Once the different spectral orders are recovered they are shifted to their correct positions in Fourier space, and the resulting image is obtained by inverse Fourier transformation. Since each spectral order can be associated with a different mechanism, conventional microscopy, optical-grating structured light, physical-grating structured light, or double-grating structured light, it is a simple matter to include the appropriate diffracted orders associated with each mechanism in the reconstruction. For purposes of clarity the reconstructions presented in the following were simply summed without any weighting function. Despite the relatively large size of the matrix that was inverted, its condition number for the ideal case of  $m_o = m_p = 1$  is approximately 4, showing that good-quality data recovers images with good signal-to-noise ratio.

Experimental results presented below demonstrate the principle of the DGSIM and also show how the physical grating provides resolution enhancement. The objective used was an Olympus Plan N  $20\times$  objective with an NA of 0.4. The period of the optical grating projected onto the sample was  $2 \mu\text{m}$ , a value expected to give modest but noticeable improvement in bandwidth. The period of the physical grating was  $1 \mu\text{m}$ . The substrate with the physical grating was sprinkled with fluorescent beads of  $1 \mu\text{m}$  diameter [FluoSphere carboxylate-modified microsphere, Crimson fluorescent (625/645) Invitrogen]; since the nanoparticles making the grating were considerably smaller than the bead diameter, the effective diameter of the beads is narrowed, because most of the fluorescent excitation emerges from the small region

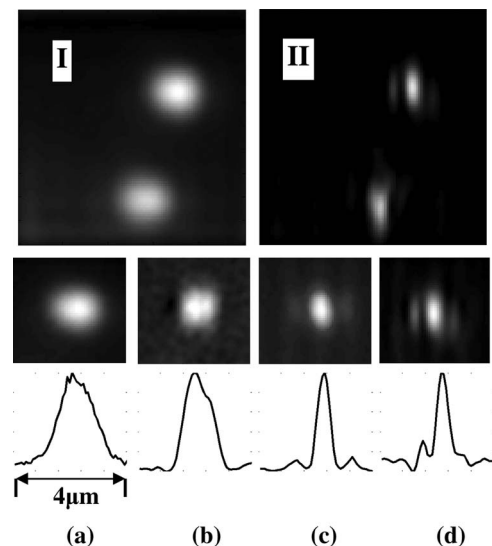


Fig. 3. Images of two fluorescent beads obtained with (I) a conventional bright field microscope and (II) with the double-grating system, both images  $9 \mu\text{m}$  in width. Second row, intermediate processing (top right particle only); third row, cross-sectional profiles of the distributions in the second row. (a) Conventional microscope, (b) optical grating only, (c) physical grating only, (d) double grating.

**Table 1. Summary of the FWHM Obtained by Applying Different Enhancement Mechanisms**

Enhancement Indicator	No Enhancement	Optical Grating	Physical Grating	Double Grating
FWHM of image in $x$ direction	1250 nm $\pm$ 50 nm	950 nm $\pm$ 50 nm	650 nm $\pm$ 50 nm	540 nm $\pm$ 50 nm
Normalized FWHM	1	0.76	0.52	0.43

that overlaps the near field of the LSPR. Indeed, some of the particles that we imaged exhibited improvement corresponding to both the physical and the optical grating, whereas others showed PSF narrowing corresponding to the optical grating only; we attribute this to the fact that they were not visible to the field of the physical grating, and moving to tighter arrays (as discussed in the summary) will produce a more densely structured field, which will help overcome this problem. This issue is a physical manifestation of the fact that we performed the reconstructions based on the assumption that the illumination is sinusoidal; although this is a good approximation for the optical grating, it is not for the physical grating, which contains harmonics resulting in a strongly peaked intensity at the position of the nanoparticles. This means that certain spurious frequencies are introduced into the reconstruction, resulting primarily from the harmonics of the grating frequency. These account for the fact that the full spectral extension is observed only at regions where the field from the physical grating changes substantially.

Figure 3 shows images of two fluorescent beads. (I) is obtained without any enhancement, and (II) is with the double grating. The second row concentrates on one of the two particles to illustrate the intermediate processing stages, showing images obtained with no enhancement, optical-grating enhancement only, physical-grating enhancement, and double-grating enhancement. The reduction in the PSF applies in one direction only. These results are tabulated in Table 1.

We have shown experimentally that an optically addressed physical grating based on particle LSPR can be used to provide PSF narrowing. The spatial phase of the structured light coming from the lithographic array can be changed without moving the particles simply by adjusting the polarization of the incident light. The period of this grating is not limited by diffraction. We have also shown how two gratings act together to further increase the bandwidth. There are still very significant technical challenges that need addressing; most are centered around further development of the physical grating. The use of a coarse grating necessary to demonstrate the movement meant that the particles were separated so that

the field was somewhat inhomogeneous. The coupling of field between closely spaced nanoparticles will produce a much more continuous distribution that will exhibit uniform spectral extension.

The use of polarization provides an excellent way of moving the grating but in one direction only; this problem may be addressed using concepts discussed in [8], where changing the incident angle or wavelength of excitation will give the additional degrees of freedom necessary to move the grating in two dimensions.

Another issue relates to the minimum achievable grating period. Although the method presented here is only one possibility, it should be noted that small particles show lower contrast between the long- and short-axis resonances. Nevertheless, this approach should still allow grating periods less than 100 nm to be used, provided interactions between the metallic nanoparticles are considered. Such periodicities when combined with an optical grating give potential bandwidth extension up to a factor of 5.

Future developments in plasmonics are expected to provide the technologies to exploit the concepts discussed in this Letter to the fullest extent.

We wish to acknowledge the financial support of the Engineering and Physical Science Research Council (EPSRC) through grants EP/C534689, EP/C534697.

## References

1. R. Heintzmann and C. Cremer, *Proc. SPIE* **3568**, 185 (1998).
2. M. G. Somekh, K. Hsu, and M. C. Pitter, *J. Opt. Soc. Am. A* **25**, 1319 (2008).
3. R. Heintzmann, T. M. Jovin, and C. Cremer, *J. Opt. Soc. Am. A* **19**, 1599 (2002).
4. A. Sentenac, K. Belkebir, H. Giovannini, and P. C. Chaumet, *Opt. Lett.* **33**, 255 (2008).
5. M. Cheng and H. Zhang, "Apparatus and method for super-resolution optical microscopy," international patent application WO 2005/078382 A1 (August 25, 2005).
6. Z. Liu, S. Durant, H. Lee, Y. Pikus, N. Fang, Y. Xiong, C. Sun, and X. Zhang, *Nano Lett.* **7**, 403 (2007).
7. G. Zorinants and W. L. Barnes, *New J. Phys.* **10**, 105002 (2008).
8. A. F. Koenderink, J. V. Hernandez, F. Robicieux, L. D. Noordam, and A. Polman, *Nano Lett.* **7**, 745 (2007).